Design and Control of a Robotic Leg with Braided Pneumatic Actuators

Robb W. Colbrunn, Gabriel M. Nelson, Roger D. Quinn
Case Western Reserve University
Cleveland, Ohio 44106
http://biorobots.cwru.edu

Abstract

A four-DOF planar robotic leg actuated with McKibben artificial muscles was designed, constructed, and controlled. Both position and passive stiffness were independently controllable at each joint. The tunable passive stiffness properties of the actuators provided stable, forward walking for the robot. A benefit of passive joint stiffness is energy efficiency. Results indicate that the leg may be capable of walking on a horizontal plane with its control valves off 90% of the time. The muscle-like properties of these actuators, including high strength-to-weight ratio, tunable passive stiffness, and self-limiting force output, make them well suited for legged robots.

1. Introduction

A Braided Pneumatic Actuator (BPA) otherwise known as a McKibben artificial muscle or Rubbertuator [9] is a device patented by Gaylord [8] and used by McKibben [13] in the late 1950's as an orthotic appliance for polio patients. In recent years, robotics engineers have begun to rediscover these fascinating devices, and use them as actuators for robots [2], [10]. They are particularly promising for legged robots because of their muscle-like properties such as tunable stiffness, high strength to weight ratio, structural flexibility, and self-limiting force output.

A robotic leg was built to provide a platform for testing control strategies for braided pneumatic actuators. We desired to make it as simple as possible, but to simulate legged locomotion, it had to alternate between stance (load phase) and swing (return phase). A four degrees of freedom (DOF) planar motion leg was designed, including two rotational joints, each actuated by an antagonistic pair of BPA. Similar to muscle, these actuator pairs can independently apply a torque and a stiffness to a joint. Therefore, sensing position only is not adequate for controlling a joint and we measure joint angle and force output of each of the two antagonistic tensile actuators.

2. Leg Design

The robot configuration shown in Fig. 1 is similar to a biped leg, thus the main joints and links are referred to as the hip, knee, femur and tibia. The leg was able to alternate between swing and stance and carry a load.

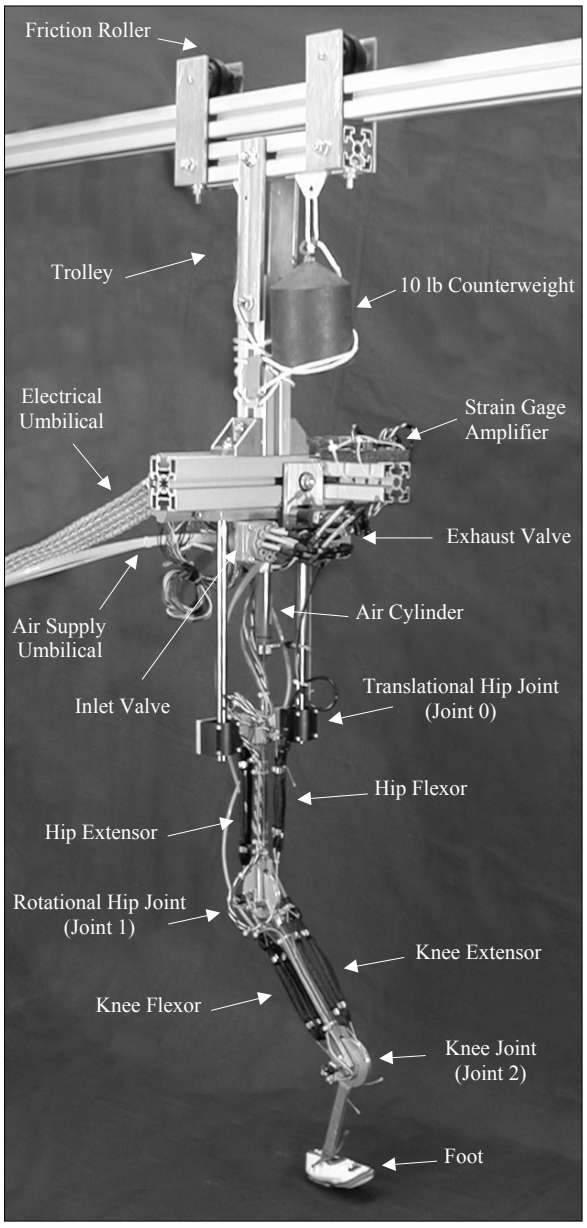

Figure 1: Labeled photograph of the complete leg

Antagonistic pairs of braided pneumatic actuators were used to drive the two rotational joints, and an air cylinder was used to drive the prismatic vertical DOF at the hip. The leg was mounted to a trolley that rolled along a track

to allow for forward motion of the robot. A 10 lb counterweight and a friction roller were added to resist motion and simulate the robot's body. The four degrees of freedom were: 1) the unactuated linear trolley motion on the track; 2) the vertical linear motion actuated by the air cylinder; 3) the rotational hip motion; and 4) the rotational knee motion. However, the air cylinder on the vertical joint was not controlled in the experiments discussed in this paper. Pressure was maintained on one side to cause it to remain extended.

The air cylinder rod at Joint 0 was attached to two linear bearings that constrained the leg to translate vertically. The rod threaded into the body link. The actuators on the body rotated the hip, or Joint 1, and those on the femur rotated the knee, or Joint 2. The foot was connected to the tibia at a passive ankle joint.

Shadow Robot Company manufactured the actuators used in this work [14]. The cylindrical center section of the actuators in Figure 2 are ⌀¼" x 3.85" long when fully stretched. To increase the force capability of the leg, the actuators were implemented in groups, two actuators to flex each joint and two to contract it.

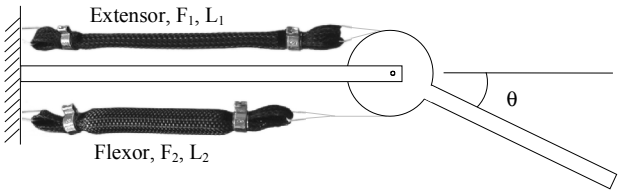

Figure 2: Schematic of a rotational joint actuated by an antagonist pair of McKibbens

Each joint was designed to be actuated by an antagonistic pair of BPA groups. This resulted in joints with tunable passive stiffness, which is a muscle-like feature that is of great benefit to legged robots [1]. Increasing the pressure in both actuators increases the joint stiffness. This is analogous to increasing activation level in an antagonistic pair of muscles. For example, Watson et al. [16] have shown that in cockroach locomotion, there is antagonistic muscle activation just before foot plant.

3. Control Architecture and Control Laws

Caldwell et al. used pulse width modulation (PWM) with position sensing and adaptive control for BPA [2]. Tondu et al. controlled both position and stiffness of BPA using servo valves and a pressure control loop [15]. This work builds upon what has been learned in the control of Robot III in the CWRU Biorobotics Laboratory [11] [12]. Robot III is actuated with double acting air cylinders, which are activated using three-way valves. Pulse width modulation (PWM) varies the pressure in the cylinders. With 3-way valves the actuator chambers can never be sealed. Therefore, the robot consumes much air during operation. For autonomy, we seek to decrease the amount of compressed air necessary to operate a robot. Instead of using two 3-way valves to control each joint as in Robot III, four 2-way valves are used to control each of the rotational joints in the leg. For each actuator group, one valve is for the air inlet, and the other is for exhaust. Unfortunately, this doubles the number of valves onboard the robot, but air can be trapped and the robot can benefit from the passive properties of BPA.

The next step was to develop a control scheme that only opened one valve of an actuator group at a time, either the inlet, or the exhaust. In doing this, the control idea was shifted from that of controlling air pressure to controlling air mass. If activation was desired, then the inlet valve was opened to increase the mass of air in the actuator. To relieve the actuator, then the exhaust valve was opened. The hardware control system is shown in Fig. 3.

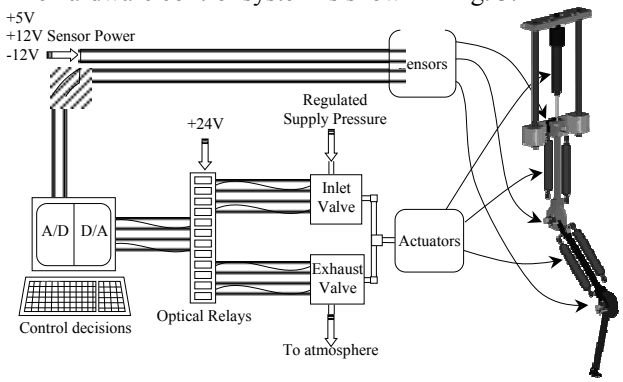

Figure 3: Hardware System Overview

The control algorithm was hierarchical (Fig. 4). A high-level controller generated the joint trajectories, performed inverse kinematics, and modulated control gains as a function of the sensory feedback signals. Whereas, a low-level controller made decisions based on the desired values given to it by the high-level controller. It performed proportional control and PWM output duty cycles that were communicated to the valves.

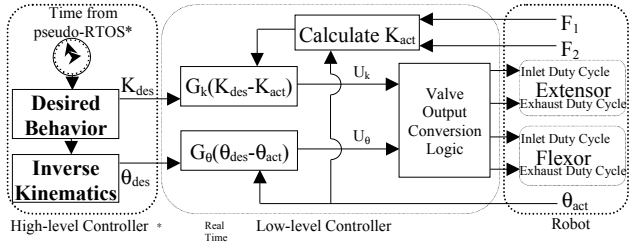

Figure 4: Block diagram of the control algorithm

In the low-level system, one law controlled joint angle, and the other controlled joint stiffness. These were designed to interact in a way that reduced the consumption of air. The extensor and flexor actuators were numbered 1 and 2, respectively. When the flexor contracted, θ increased as shown in Fig. 2.

The valve output conversion logic (Fig. 4) is what converted the two-space control outputs, U_k and U_θ, into the four-space signals to the valves. This conversion method quickly converted U_k and U_θ to valve duty cycles and also conserved air. The valve output conversion logic is as follows:

$$\text{Extensor Inlet Duty Cycle} = U_k - U_\theta \quad (1)$$

$$\text{Extensor Exhaust Duty Cycle} = -U_k + U_\theta \quad (2)$$

$$\text{Flexor Inlet Duty Cycle} = U_k + U_\theta \quad (3)$$

$$\text{Flexor Exhaust Duty Cycle} = -U_k - U_\theta \quad (4)$$

When an increase in θ is desired, the flexor inlet valve operates at a duty cycle governed by U_θ. The extensor exhaust valve also operates at the same duty cycle. When an increase in stiffness is desired, both inlets operate at a duty cycle governed by U_k. When a decrease in stiffness is needed, both the exhausts operate at U_k. When U_k and U_θ are added according to (1)-(4), both flexor valves have the same duty cycle, but a different sign. The same thing is done with the extensor valves. To prevent both valves from opening at the same time, and wasting air, all negative duty cycles are set to zero. The control laws are:

$$U_k = G_k\left(K_{des} - K_{act}\right) \quad (5)$$

$$U_\theta = G_\theta\left(\theta_{des} - \theta_{act}\right) \quad (6)$$

where G_k = stiffness control gain, G_θ = angle control gain, θ_{act} = Measured angle, θ_{des} = desired angle, K_{act} = measured stiffness, and K_{des} = desired stiffness. The control gains were chosen by trial and error.

To implement (5), an equation for K_{act} was needed given the measurements of the forces in the actuators. The derivation of K_{act} [4][5] is based on the force-length relationship derived by Chou and Hannaford [3]. Actuator force, F, is a function of the internal gage pressure, P_g, and the McKibben cylindrical parameters; thread length, b, the number of turns for a single thread, n, and the actuator length L:

$$F = \frac{P_g b^2}{4\pi n^2}\left(\frac{3L^2}{b^2} - 1\right) \quad (7)$$

The linearized stiffness, k, is calculated by taking a derivative of the force with respect to length:

$$k = \frac{6F}{\left(3L - \frac{b^2}{L}\right)} \quad (8)$$

The stiffness of an individual actuator is given by (8). The stiffness at the joint, K_{act}, is the summation of the stiffness of the two antagonistic actuators, k_1 and k_2, multiplied by the square of their respective moment arms. Note that each muscle group consists of two actuators. The equivalent stiffness of two actuators is twice the stiffness of one actuator.

When the proportional control laws (5) and (6) are combined with the valve output conversion logic, they have an imbedded integral control property. Suppose the leg is physically restrained not to rotate from an angle of 15°, and yet the desired angle is 20°. The flexor inlet valve will put more air into the actuator while the extensor exhaust valve also opens at a rate given by U_θ. The next time the control calculation is made, there will still be a 5° error. Therefore, the same U_θ will again open both the flexor inlet and extensor exhaust valves. This loop will continue until the flexor actuator is filled to the supply pressure, and the extensor pressure is atmospheric, which provides the maximum joint torque possible. Therefore, as error accumulates over time, the joint torque is increased in an effort to reduce it. The same holds true for stiffness errors.

4. Walking Results

The joint angles, actuator forces, calculated stiffnesses, and commanded duty cycles were recorded while the leg walked. Post processing produced ground reaction forces and foot motions.

Figure 5 shows the y-coordinate of the ground to be about –13". The 0.5" difference between the desired and actual was intentional. The proportional controller only produces a force to lift and propel the robot if there is an error. Figure 5 shows poor foot position control, but during walking, precise position control is not as important as stable actions that cause forward motion. Figure 5 includes data from four walking cycles overlaid. The actual foot path is smooth and repeated. The one deviant path in the

middle was the foot motion from its initial resting position. Note that joint angles, not foot path, were being controlled.

The zero positions and sense of the joint angles are shown in figure 6. Figure 7 shows the desired and actual joint angles versus time. The small time delay shift characteristic of proportional control is apparent. With the exception of a small section of the swing phase of Joint 2, all of the desired joint angles were within the possible joint ranges of motion. However, Figure 7 shows that the joints did not reach these limit positions. This can be attributed to the joint stiffness/range of motion trade-off. If both antagonist actuators are filled with supply pressure air to achieve a large desired stiffness, the joint can not move while that stiffness is maintained. This explains why the foot did not follow the desired motion during the swing phase (Fig. 5). In Fig. 7 there is also a larger than normal angle error during the propulsion phase. This was due to the planned 0.5" foot y-position error. Figure 7 shows that the position control scheme could be improved by putting the desired values within the attainable ranges of motion, which are stiffness dependent. Small oscillations are also apparent in the hip joint at the beginning of each swing phase.

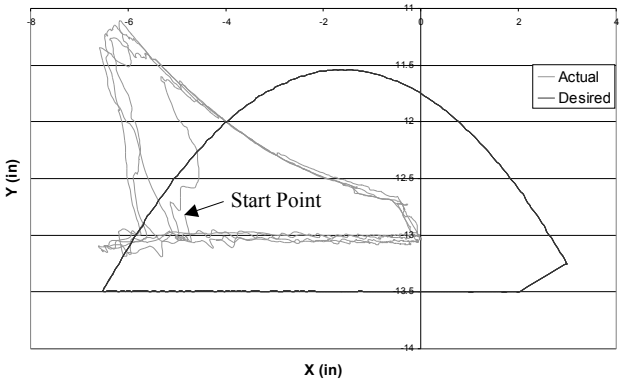

Figure 5: Desired and actual x-y foot paths.

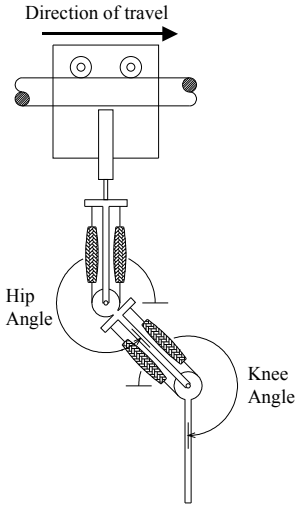

Figure 6: Joint angle definitions

The maximum actuator force was nearly 30 lbs, which is the maximum output of a muscle group (two actuators). As was expected, during the swing phase the antagonistic actuator forces were nearly the same to satisfy the commanded stiffness requirement (Fig. 8). During the propulsion phase, these actuator forces deviated in opposite signs as the ground applied external forces. Figure 8 also shows that only the Hip Extensor actuator was being used to its maximum capacity. This meant that adding another actuator in the hip flexor bundle could increase the maximum load capacity of the leg.

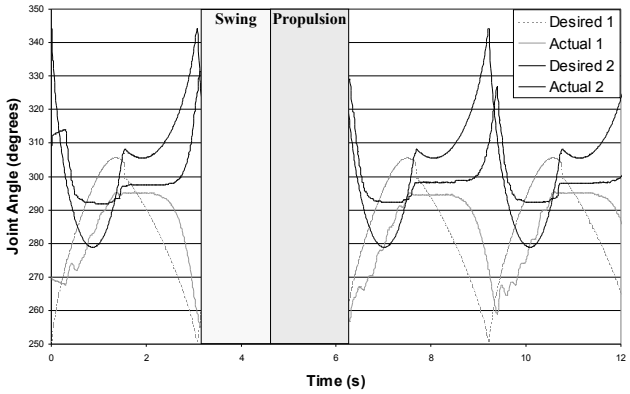

Figure 7: Desired and actual joint angles vs. time.

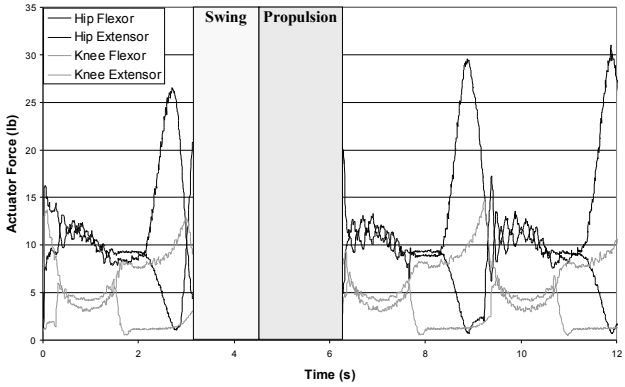

Figure 8: Actuator force vs. time

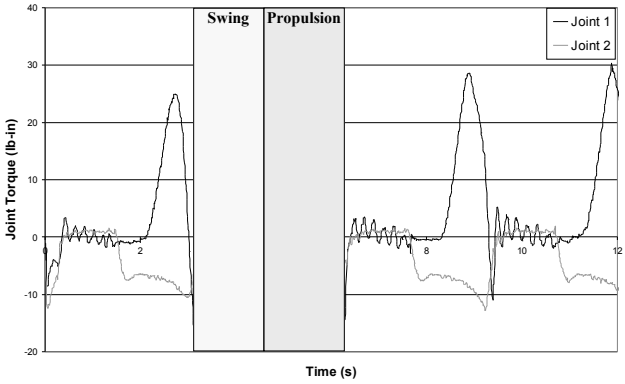

Figure 9: Joint torque vs. time

The joint torques were calculated by subtracting the output of the antagonistic force sensors (Fig. 9). During the swing phase the torques are nearly zero. Only the inertial and gravity effects caused a difference in actuator force. The slight oscillation of the hip joint was again apparent in the torque data. Also, notice the slope of the torque signal during the swing phase. This was due to the change in gravity induced torque as the femur and tibia orientations changed. When the foot was set on the ground, the normal and friction forces at the ground applied an external moment to the leg. The actuators carried these moments with magnitudes shown in the propulsion phase of Fig. 9.

The joint position and torque data were used to determine the normal y and longitudinal x forces at the foot (Fig. 10). These calculations ignored inertial and gravity effects, which caused some false reaction forces during the swing phase. However, these were minimal in relation to the forces during propulsion. Therefore, if the ground reaction forces are desired as feedback in a control algorithm, ignoring the inertial terms will provide accurate results. The minimal effect inertia had during swing also suggests that the ground reaction forces during propulsion were accurate.

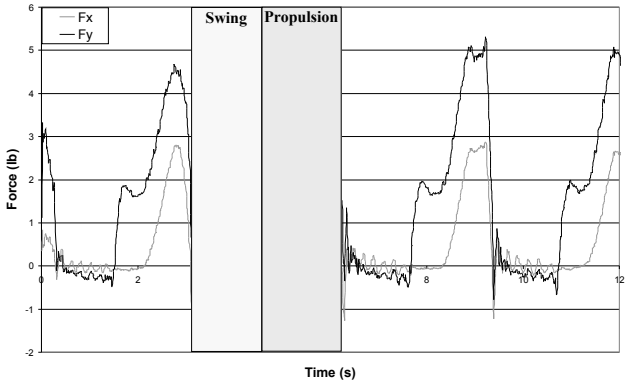

Figure 10: Ground reaction forces during walking.

A goal of this work was to have the leg motion be produced by passive mechanisms as much as possible. A measure of this is the time that the valves are open. Minimizing the valve open time reduces air consumption, which is important for autonomy. The commanded duty cycles were recorded during the walking motion and plotted as a function of time.

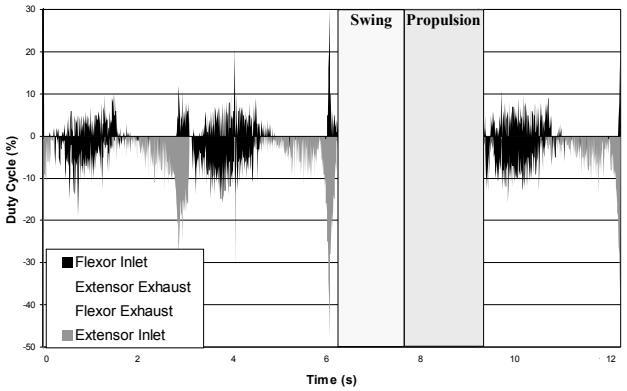

Figure 11: Hip joint valve duty cycles vs. time

In Figs. 11 and 12, the flexor valve duty cycles were plotted in the positive domain, and the extensor valve duty cycles were plotted in the negative domain. The flexor duty cycles for the knee were much larger than those for the hip. The large knee flexor inlet duty cycles were a by-product of the fact that during the swing phase the desired joint angle was beyond its possible range of motion. If the desired angle had been achievable, we expect that the flexor inlet duty cycles would have been much smaller. The largest duty cycle in Figure 12 is for the flexor exhaust. The valve was opened in order to reduce the joint stiffness, however, air was not wasted and autonomy was not compromised because the flexor inlet duty cycles were much less than the flexor exhaust. Therefore, for most of the propulsion phase the flexor actuator contained atmospheric pressure air even though the exhaust valve was still being operated. This phenomenon is also

apparent in Figure 11. The flexor inlet valve duty cycles were less than the exhaust.

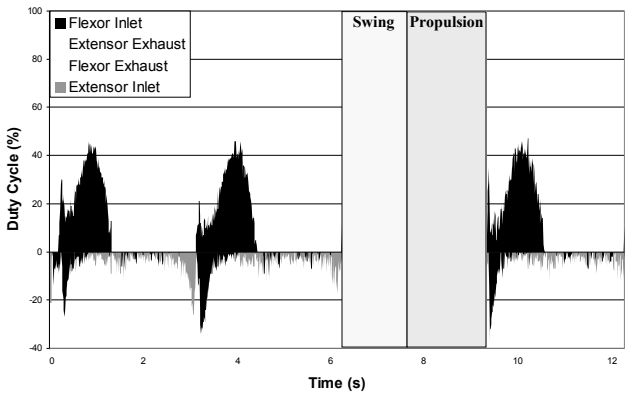

Figure 12: Knee joint valve duty cycles vs. time

The duty cycles for the valves were combined to quantize a simple indicator of the "passiveness" of the system. An average duty cycle value is indicative of the consumption of air. It also provides an estimate of how much of the control was active versus passive. Table 1 shows the average duty cycle for each valve. By design, the inlet and exhaust valves never operate at the same time. Therefore, the passiveness for each actuator is calculated by subtracting the sum of these values from 100%. Because the flexor and extensor valves operate at the same time, the passiveness at each joint is equal to the passiveness of the least passive of the flexor or extensor. Also, the total robot passiveness is equal to the passiveness of the least passive joint.

Table 1: Passiveness and Average Duty Cycles of Each Valve

	Flexor		Extensor		
Joint	Inlet	Exhaust	Inlet	Exhaust	Passiveness
Hip	2%	4%	3%	3%	94%
Knee	11%	23%	2%	3%	66%
				Total Passiveness	66%

With the current configuration, the robot passiveness was 66%. Table 1 also suggests that if the knee flexor valve's duty cycles were reduced by maintaining the desired joint angle within its possible range of motion, in accordance with the discussion above, the robot passiveness might be as high as 94%. This desirable passiveness can be attributed to three things. First, the two 2-way valves provide a convenient method to trap air in the actuators. Second, the valve output conversion logic does not allow both inlet and exhaust valves to be open at the same time and, thereby reduces air consumption. Third, the length-dependent stiffness of braided pneumatic actuators allows an antagonist BPA to compensate, about a joint, for the dropping stiffness of a contracting BPA.

5. Motion Results

Other tests were performed to better understand the capabilities of the robot leg. The first test was to double the rate at which the desired trajectory was generated to test tracking at a higher speed. Figure 13 is a comparison plot of desired and actual joint angles.

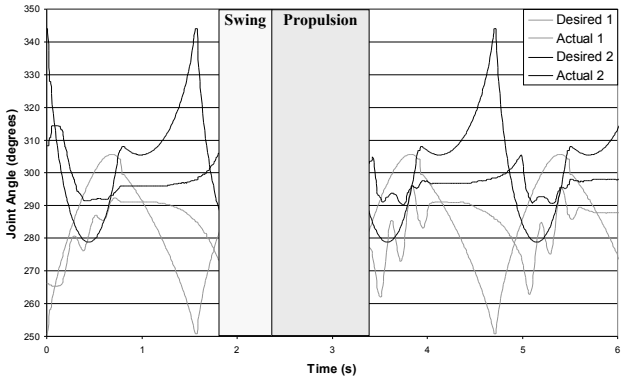

Figure 13: Desired and actual joint angles vs. time for fast walking

Figure 13 shows oscillations at both joints, with substantial ones at the hip joint. However, the leg was stable because of the passive properties of the actuators. There was also another downside to the faster walking. In one cycle, the trolley traveled forward only 21", less than half that of the normal walking motion, 60". We evaluated two possible reasons for this degradation in performance at faster walking speeds. First, we tested the leg to determine if it was capable of performing rapid motions by having it follow a kicking trajectory (Fig. 14).

Figure 14 suggests that the leg response time is good. From the retracted position to the extended position, the forward motion took place in about 90 ms. To achieve such a quick response time, the desired stiffness and control gains were modulated during the motion. The control gains for the normal walking motion were too low for the leg to respond this quickly. This suggests that it is beneficial to design the high level controller to be capable of modulating all the system parameters. It is also apparent from Figure 14 that oscillations were present in the system. This suggests that the reason the fast trajectories degraded the walking performance was not the speed capability of the actuators and valves, rather, there was not enough damping in the system. Higher angle control gains are needed to produce better trajectory following, but higher control gains cause the leg to oscillate more. To dissipate vibrational energy at the joint, we could physically place a damping mechanism on the leg, or add a derivative control term in software. The passive moment in human joints from dissipative effects has been estimated to be

proportional to the joint velocity raised to the 0.2 power [6]. Garcia et al. [7] report that damping in animal joints is a function of the scale of the animal.

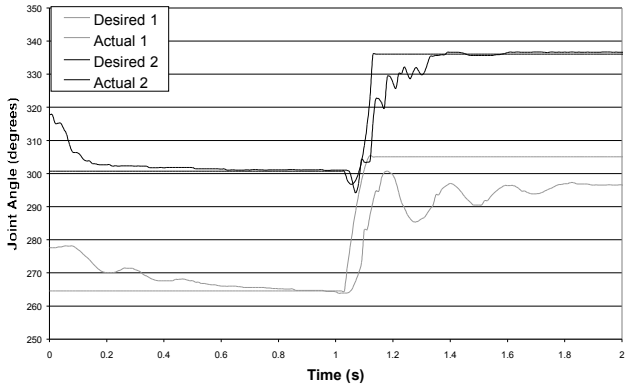

Figure 14: Desired and actual joint angles vs. time for kicking trajectory

6. Conclusions

This paper presents a planar robotic leg that walks using braided pneumatic actuators as the prime movers. The leg moves on a horizontal track with its control valves off for 66% of the time. If the desired trajectory of the knee were changed to reflect the joint limits, results indicate that this value could be higher than 90%. Therefore, much of the control system is imbedded in the passive mechanics of the robot. This passiveness simplifies the control problem and reduces the energy needed to operate the robot, both of which are important for autonomy. Slow, deliberate motions of this leg are possible, but so are rapid motions such as in the kicking test. Modulation of the system parameters in the controller make this possible. Fast cyclic motions require the addition of a damping mechanism. Braided pneumatic actuators show great promise. Their muscle-like high strength-to-weight ratios, tunable passive stiffness, structural flexibility, and self-limiting properties make them good candidates for use in legged robots.

Acknowledgements

This work was supported by the Office of Naval Research N0014-99-1-0378 and DARPA DAAN02-98-C-4027.

References

[1] Alexander, R. McN., (1990) Three uses for springs in legged locomotion. *Int. J. of Robot. Res.*, 9 (2), 53-61.

[2] Caldwell, D.G., Medrano-Cerda, G.A., and Goodwin, M.J. (1995) Control of Pneumatic Muscle Actuators. *IEEE Control Systems Journal*, 15(1):40-48.

[3] Chou, C.P., B. Hannaford, (1996). "Measurement and Modeling of McKibben Pneumatic Artificial Muscles," "*IEEE Transactions on Robotics and Automation*," Vol. 12, No. 1, pp. 90-102.

[4] Colbrunn, R., (2000) *Design and Control of a Robotic Leg with Braided Pneumatic Actuators*, M.S. Thesis, Case Western Reserve University, Cleveland OH.

[5] Colbrunn R., Nelson G.M., Quinn R.D, (2001). "Modeling of Braided Pneumatic Actuators for Robotic Control, " IEEE IROS, HA.

[6] Esteki, R.M. and Mansour, J.M., (1996). "An experimentally based nonlinear viscoelasatic model of joint passive moment," *J. of Biomech*. V. 29, pp 443-450.

[7] Garcia, M., Kuo, A., Peattie, A., Wang, P. and Full, R., (2000). "Damping and size: Insights and biological inspiration," *Int. Symp. On Adaptive Motion of Animals and Machines*, August 8-12, 2000.

[8] Gaylord, R.H., (1958) Fluid actuated motor system and stroking device. U.S. Patent 2,844,126, July 22, 1958.

[9] Inoue K. (1987) Rubbertuators and Applications for Robots. Proceedings of the 4th Symposium on Robotics Research, Tokyo, 57-63.

[10] Klute, G.K., J.M. Czerniecki, and B. Hannaford, "McKibben Artificial Muscles: Pneumatic Actuators with Biomechanical Intelligence," Proceedings of the IEEE/ASME 1999 International Conference on Advanced Intelligent Mechatronics (AIM '99), Atlanta, GA, September 19-22, 1999.

[11] Nelson G.M., *Simulation and Control of a Cockroach-Like Robot*, Ph.D. Thesis, Case Western Reserve University, Cleveland OH, (in press).

[12] Nelson, G. M. and Quinn, R. D., (1999). "Posture Control of a Cockroach-like Robot," *IEEE Control Systems*, Vol. 19, No. 2, April 1999.

[13] Nickel, V.L., J. Perry, and A.L. Garrett, (1963). "Development of useful function in the severely paralyzed hand," "*Journal of Bone and Joint Surgery*," Vol. 45A, No. 5, pp. 933-952.

[14] Shadow Robot Company (2000). http://www.shadow.org.uk/products/airmuscles.shtml

[15] Tondu B., Boitier, V., and Lopez, P. (1994) Naturally Compliant Robot-arms Actuated by McKibben Artificial Muscles. Proceedings of the 1994 IEEE Int. Conf. on Systems, Man and Cybernetics, San Antonio, TX, 3:2635-2640.

[16] Watson, J. T., R. E. Ritzmann (1998) "Leg kinematics and muscle activity during treadmill running in the cockroach*, Blaberus discoidalis:* I. Slow running," "*J. Comp. Physiol. A*," Vol. 182: pp.11-22.